CORROSION SCIENCE AND TECHNOLOGY, Vol.20, No.5(2021), pp.242~248 pISSN 1598-6462 / eISSN 2288-6524
[Research Paper] DOI: https://doi.org/10.14773/cst.2021.20.5.242

Failure Investigation of Fire-Side Water-Wall Tube Boiler

M. C. Fatah[1,†], D. Agustiadi[1], and A. W. Pramono[1,2]

[1]*Mechanical Engineering Department, Institut Teknologi PLN (IT PLN), Jakarta, Indonesia*
[2]*Research Centre of Materials and Metallurgy, Indonesian Institute of Sciences, Serpong, Indonesia*
(Received June 29, 2021; Revised August 11, 2021; Accepted September 20, 2021)

Unforeseen failures of boilers in power plants may affect the continuation of electricity generation. Main failures in boilers are influenced by the tube material, tube position, boiler service temperature and pressure, and chemical composition of the feed water and coal. This investigation was intended to find answers on the causes and mechanism of failure of the fire-side boiler water-wall tubes, due to perforation and corrosion. The tube conformed to the material requirements in terms of its chemical composition and hardness. Microscopic examination showed ferrite and pearlite indicating no changes in its microstructure due to the temperature variation. SEM test showed a single layer and homogenous film density particularly on the area far from perforation. However, layers of corrosion product were formed on the nearby perforation area. EDX showed that there were Na, Ca, S, and O elements on the failed surface. XRD indicated the presence of Fe_2O_3 oxide. The failure mechanism was identified as a result of significant localized wall thinning of the boiler water wall-tube due to oxidation.

Keywords: *Failure, Hardness, Wall thinning, Perforation, Oxidation*

1. Introduction

Nowadays, coals are still used as one of the major sources of energy in power plant because of their capability to generate high demand of electricity. However, unforeseen failures in boilers lead to power plant shut down and discontinue of electricity generation. Main failures in boilers can be affected by the tube material, tube position, boiler service temperature and pressure, and chemical composition of the feed water and coal [1].

The corrosion of boiler tubes is one of the remaining challenges in steam power plants. Tubes failure leads to the plant shut-down, tubes repair, replacement and welding. It has also required welding inspections to avoid welding defects. All these activities cause tremendous costs.

In the boiler combustion system, sodium sulphate and oxide are formed from the reaction of Na, O and S. Furthermore, these elements combine to form various types of vapours and condensed phases which deposit on the surface materials [2]. Degradation of materials occurs when these molten condensed phases destroy the natural protective oxide layer of the material surface during boiler operation [3]. The complex environment under the boiler operating condition makes it very challenging for a material to suffer all the tough situations imposed on it [1]. Therefore, understanding corrosion behaviour and mechanism on the tubes surfaces is crucial in order to prevent catastrophic incident caused by boiler failures.

A failure on fire side of water-wall tube of coal-based power plant was observed. The failure has taken place in the form of perforations and corrosion products. This investigation is intended to investigate the cause and mechanism of such failures.

2. Experimental Procedures

The failed water-wall tube boiler was analysed visually for the type of failure and its photograph was recorded. The chemical composition of failed tube was analysed using optical emission spectrometer (WAS foundry master). The hardness of the failed tube at the location closer to and away from the failed region was determined using a Rockwell hardness machine (Qualirock digital hardness tester) under a load of 100 kgf. A small piece of sample was cut from the failed region (area A in Fig. 2), polished using standard metallographic techniques, etched using

[†]Corresponding author: martin@itpln.ac.id

Fig. 1. Photograph of failed tube inside the boiler

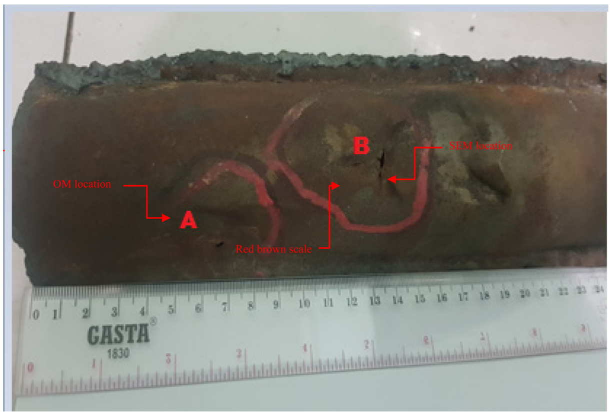

Fig. 2. Photograph of the failed tube after removed from inside boiler.

3% Nital and analysed for its microstructural features, using an optical microscope (Olympus, BX41M - LED). A scanning electron microscope (Inspect, F50) attached with energy X-ray analysis (EDAX) and XRD (Shimadzu, type 7000) were used to analyse the morphology and chemical composition of the deposit (area B in Fig. 2), to ascertain the nature of failure. The thickness of the tube near failed region was measured by a digital calliper for at least in three different locations, and the average thickness value was calculated.

3. Results and Discussion

The technical and operational parameters of the boiler are given in Table 1 and Table 2. Sulphur and sulphur dioxide were found in the coal and flue gas analysis as

Table 1. Main Economic Data and Technical Parameter of the Boiler

No	Properties	Value
1	Rated capacity	75 t/h
2	Rated superheated steam pressure	5.3 MPa
3	Rated superheated steam temperature	485 ºC
4	Feed water temperature	150 ºC
5	Boiler designed efficiency	87.3%
6	Smoke-Exhausted Temperature	150 ºC
7	Sewage Rated	2%
8	Steel Consumption of Boiler Proper (ton)	526
9	Steel Consumption of Steel Frame (ton)	145
10	Q Net air	3808 kcal/kg
11	Size coal	0-10 mm
12	Coal type	Low Calorific
13	Type	*Circulating Fluidized Bed* (CFB)

Table 2. Operating conditions of the failed boiler tube

No	Operating conditions	Value
1	Temperature (°C)	855
2	Pressure (Pa)	51.6
3	Tube thickness (mm)	6

shown in Table 3 and Table 4, respectively.

According to the manufacturer, the failed boiler tube was made of ASTM A106B steel. The chemical composition of the failed tube is shown in Table 5 [4]. It is seen that the chemical composition of tube meets the standard requirements according to ASTM A106B. The hardness measured at locations around failed region was approximately 83 HRB, which is within standard for carbon steel pipes for high temperatures application (77-83 HRB) [4]. Hence, it can be inferred that the tube conforms to the material requirements in terms of its chemical composition and hardness.

The failed water-wall tube is shown in Figs. 1 and 2. It is clearly seen that there were two perforations on the tube (A and B locations) with the approximate dimension (length × width) of 3 mm × 2mm and 10 mm × 2 mm, respectively. Thickness measurements showed significantly reduction in thickness from 6 mm to approximately 1.5 mm for A and 3 mm for B location. In addition, the

Table 3. Coal proximate analysis

Parameter	Unit	Result	Method
Total Moisture	% AR	28.07	ASTM D3302-2011
Proximate			
Inherent Moisture	% ADB	13.49	ASTM D3173-2011
Ash Content	% ADB	4.97	ASTM D3174-2011
Volatile Matter	% ADB	42.18	ASTM D3175-2011
Fixed Carbon	% ADB	39.36	BY DIFFERENCE
Total Sulphur	% ADB	0.36	ASTM D4239-2011
Gross Calorific Value	kcal/kg ADB	5808	ASTM D1989-2011
Hardgrove Grindability Index	Index Priority	63	ASTM D409/D409-2011

Table 4. Flue gas emission analysis

Parameter	Unit	Result	Requirements	Method
Nitrogen Dioxide	mg/nm^3	116	300	SNI 19-7117.5-2005
Sulfur Dioxide	mg/nm^3	64	800	SNI 19-7117.3.1-2005
Particle	mg/nm^3	39	350	SNI 19-7117.12-2005
Opacity	%	10	35	SNI 19-7117.11-2005
Hydrogen Fluoride	mg/nm^3	< 0.01	1,000	SNI 19-7117.9-2005
Hydrogen Chloride	mg/nm^3	< 0.01	70	SNI 19-7117.8-2005
Carbon Monoxide	mg/nm^3	35	100	SNI 19-7119.10-2011
Total Hydrocarbon	mg/nm^3	10	35	SNI 19-7119.13-2009
Arsenic	mg/nm^3	< 0.005	8	SNI 19-7117.20-2009
Cadmium	mg/nm^3	< 0.01	8	SNI 19-7117.20-2009
Chromium	mg/nm^3	< 0.01	1	SNI 19-7117.20-2009
Lead	mg/nm^3	< 0.01	12	SNI 19-7117.20-2009
Mercury	mg/nm^3	< 0.001	0.2	SNI 19-7117.20-2009
Thalium	mg/nm^3	< 0.01	0.2	SNI 19-7117.20-2009
Velocity	m/s	13,2	-	SNI 19-7117.1-2005

Table 5. Chemical composition comparison of failed tube and ASTM A106B

No.	Elements	Weight (%)	
		Failed tube	ASTM A106B
1	C	0.277	0.3
2	Si	0.229	0.1 min
3	Mn	0.445	0.29 – 1.06
4	P	0.026	0.035 max
5	S	0.008	0.035 max
6	Cr	0.012	0.4 max
7	Mo	< 0.005**	0.15 max

Table 5. Continued

No.	Elements	Weight (%)	
		Failed tube	ASTM A106B
8	Ni	< 0.005**	0.4 max
9	Al	0.009	-
10	Cu	0.005	0.4 max
11	Nb	< 0.002**	-
12	Ti	< 0.002**	-
13	V	< 0.002**	0.08 max
14	Fe	Balance	

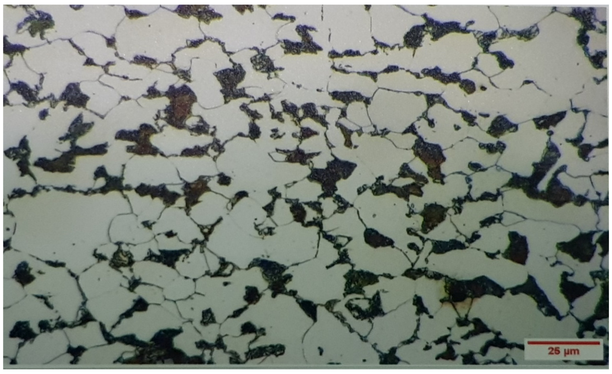

Fig. 3. Optical metallograph of the failed tube

failed surface of the tubing was covered with red-brown colour indicating iron oxide scale.

The optical micrograph prepared from fractured water-wall tube is shown in Fig. 3. The general microstructure consisted of ferrite and pearlite grain structure indicating no obvious microstructural degradation due to localized temperature variation during service.

The results of SEM micrograph are shown in Fig. 4. It is obviously seen layers of corrosion product was formed particularly on the nearby perforation area. EDAX (Figs. 5 and 6) confirmed the presence of Na, Ca, O and S elements on the corrosion product. It is believed that the presence of Na, Ca, and S comes from the fossil fuels [5].

The result of XRD is shown in Fig. 7. It is confirmed the presence of Fe_2O_3 (hematite) film on the failed tube surface.

It is well known in fire-side corrosion with corrosive species i.e. Na and S cause deposits formation on the tube surfaces and consequently severe corrosion [5]. Sodium (Na) comes from residual fuel oil along with coal which is extensively used in the energy generation system. Sodium hydroxide (NaOH) formed as a result of the condensation of vapours of sodium [6].

For the sulphur (S), it could be oxidized to SO_2 and SO_3 depending on the temperature and oxygen concentration in the boiler, Furthermore, oxidized sulphur (SO_3) reacts with NaOH producing sodium sulphate according to the following reactions [5]:

$$NaOH + SO_3 \rightarrow Na_2SO_4 + H_2O \quad (1)$$

In this study, unfortunately, the presence of Na_2SO_4 was not detected by XRD results. However, EDAX results confirmed the presence of Na, S and O elements that might indicate the presence of Na_2SO_4.

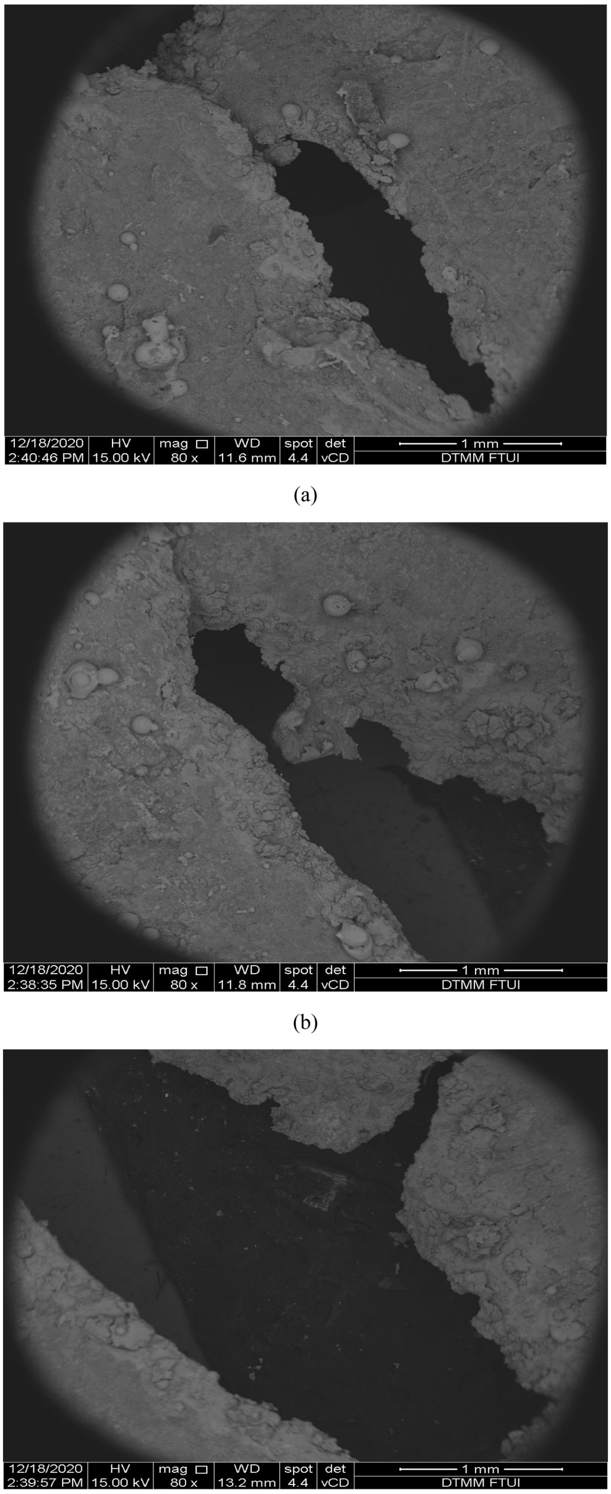

(c)

Fig. 4. Various SEM images of failed tube

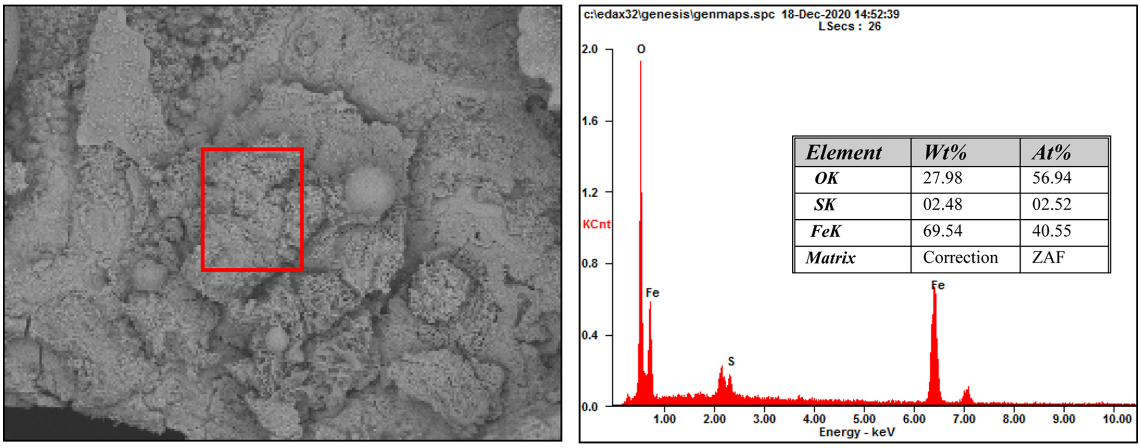

Fig. 5. SEM and EDX analysis of the failed tube at location A

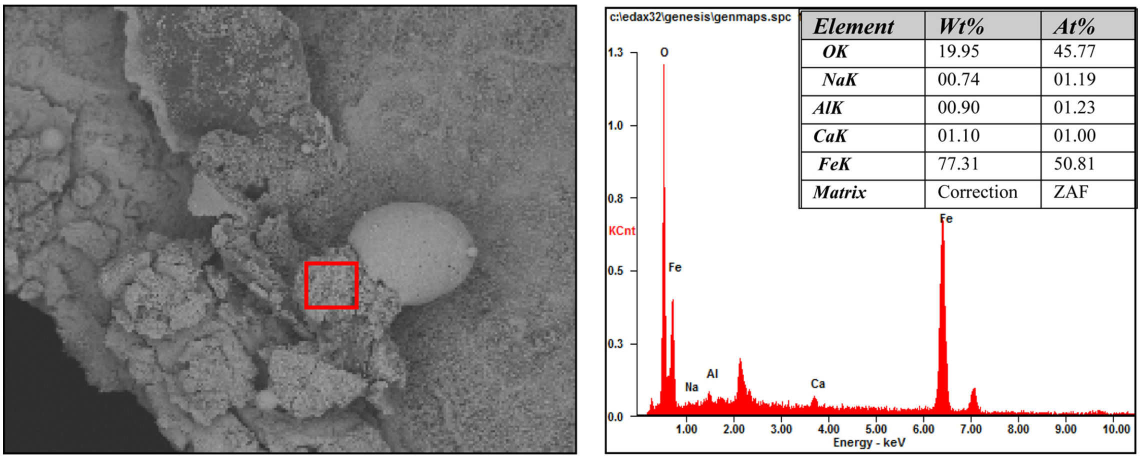

Fig. 6. SEM dan EDX analysis of the failed tube at location B

At the initial stages of boiler condition, an oxide film was formed on the external tube surface due to reaction of the steel with oxygen. Sodium sulphate then deposited on the oxide layer. Afterward, the outer surface of Na_2SO_4 layer began to become sticky and adsorbed fly ash particles dissolving the oxide layer of metal and increasing the deposit thickness [7]. By increasing deposit thickness, the temperature gradient also increased gradually. High temperature (± 600 ºC) caused the deposits and oxide layers vanished from the surface and hence further oxidation of the metal occurred [7,8]. Oxidation corrosion of steels was easy to happen due to high affinity of oxygen to react with steel to form oxides. The kinetic of oxidation was higher at high temperatures than room temperature [9]. The simple schematic diagram of boiler fire side tube corrosion could be seen in Fig. 8.

The anodic and cathodic reactions are as follow:

$$Fe \rightarrow Fe^{2+} + 2e^- \qquad (2)$$

At cathodic sites, a variety of reactions can take place and employ the generated electrons. Two most probable reactions are [5,7]:

$$O_2 + 4e^- \rightarrow 2O^{2-} \qquad (3)$$

$$SO_4^{2-} + 8e^- \rightarrow S^{2-} + 4O^{2-} \qquad (4)$$

Furthermore, Fe_2O_3 is formed by the following reactions [10]:

$$2Fe^{2+} + 3O^{2-} \rightarrow Fe_2O_3 \qquad (5)$$

or

$$2Fe + 3H_2O \rightarrow Fe_2O_3 + 3H_2O \qquad (6)$$

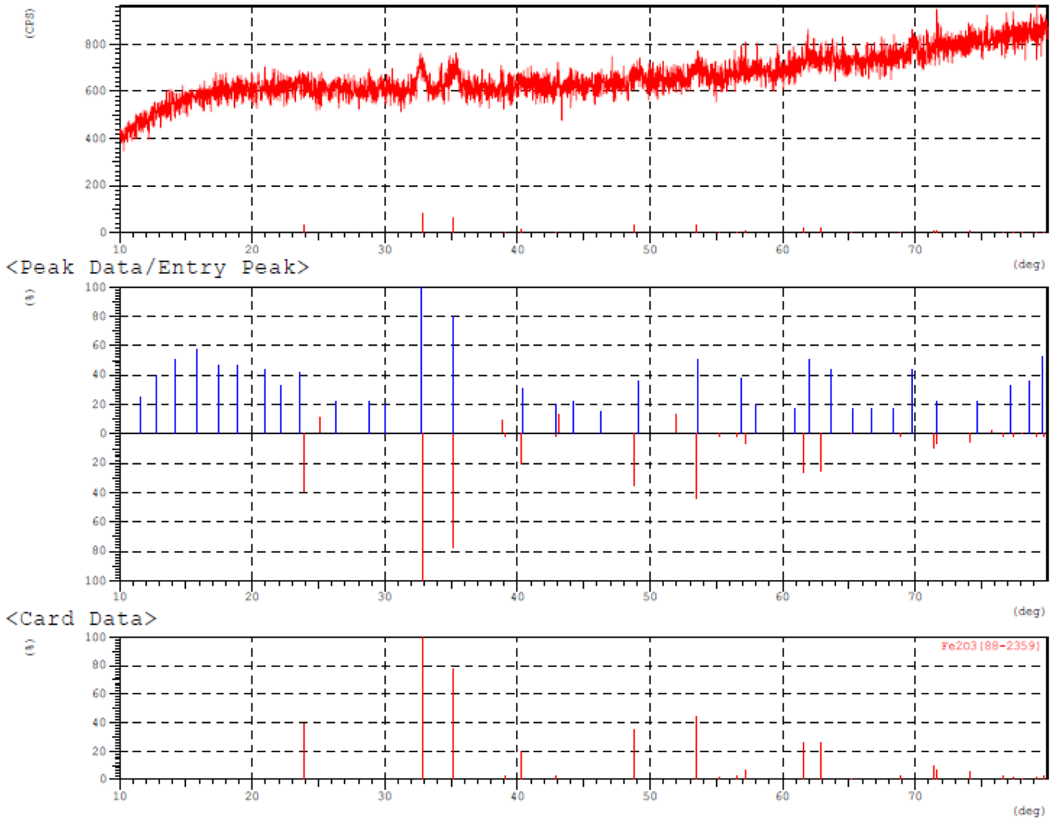

No.	Card	Chemical Formula	S	L	WT%	d	I	R
		Chemical Name (Mineral Name)		Dx		S.G.		
1	88-2359	Fe_2O_3	1.000	0.565(13/29)		0.650	0.631	0.232
		(Hematite)		5.09		R-3c		

Fig. 7. XRD results of film formed on the failed tube

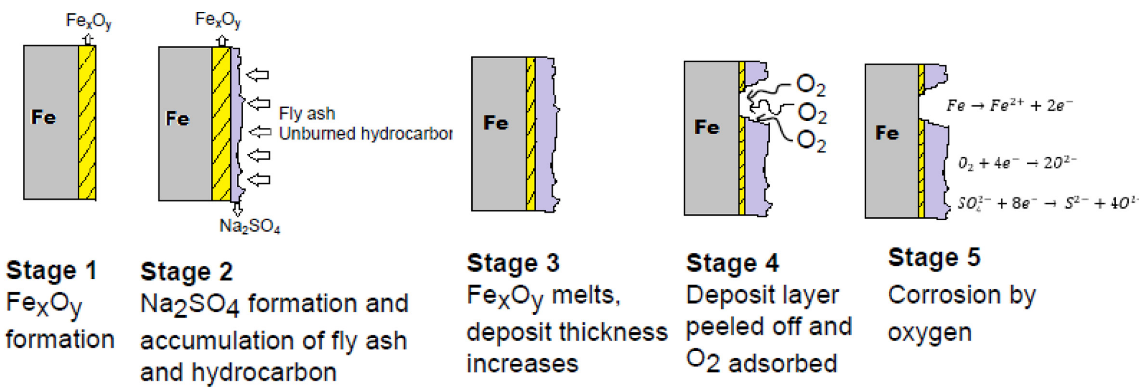

Fig. 8. The schematic diagram of fire side wall tube corrosion

4. Conclusions

The boiler water-wall tube was found failed on the fire-face side. Through examination it is found that the composition of the material and the hardness of the tube meets the requirements of the standards material of ASTM A106B. The microstructure of the failure tube consists of ferrite and pearlite, which indicate no changes on its microstructure. The fire-facing side of the tube was observed to have experienced significant wall thinning. The corrosion products of the wall tube are mainly iron oxide (Fe_2O_3). The result shows that high temperature gradient causes the deposits and oxide layers vanished from the surface and hence further oxidation of the metal occur.

References

1. N. S. Harding and D. C. O'Connor, Ash deposition impacts in the power industry, *Fuel Processing Technology*, **88**, 1082, (2007), Doi: https://doi.org/10.1016/j.fuproc.2007.06.018
2. S. S. Chatha, H. S. Sidhu, and B. S. Sidhu, High temperature hot corrosion behaviour of NiCr and Cr_3C_2-NiCr coatings on T91 boiler steel in an aggressive environment at 750 ºC, *Surface and Coatings Technology*, **206**, 3839, (2012). Doi: https://doi.org/10.1016/j.surfcoat.2012.01.060
3. E. Labuda, K. J. Shields, and D. A. Cline, *Corrosion*, Fireside corrosion in coal-and oil-fired units: failure mechanisms and methods of prevention, p. 00234, Florida (2000).
4. W. Stichel, *Handbook of comparitative world steel standards;* vol. 48, no. 6, American Society for Testing and Materials, PA, USA (1996).
5. M. Asnavandi, M. Kahram, M. Rezaei, and D. Rezakhani, Fire-Side Corrosion: A Case Study of Failed Tubes of a Fossil Fuel Boiler, *International Joursnal of Corrosion*, **2017**, 1, (2017). Doi: https://doi.org/10.1155/2017/7367046
6. H. Tran, P. Centre, and A. Chemistry, RECOVERY BOILER FIRESIDE DEPOSITS AND PLUGGING, pp. 1-13, [Online]. Available: https://www.tappi.org/globalassets/documents/awards/4-7.pdf
7. W. T. Reid, *External corrosion and deposits; boilers and gas turbines*, Elsevier Ltd., New York (1971).
8. J. Purbolaksono, F. Tarlochan, M. M. Rahman, N. F. Nordin, and B. Ahmad, Failure investigation on reheater tube due to deposit and wall thinning, *Journal of Failure Analysis and Prevention*, **9**, 365 (2009). Doi: https://doi.org/10.1007/s11668-009-9250-1
9. S. W. Liu, W. Z. Wang, and C. J. Liu, Failure analysis of the boiler water-wall tube, *Case Studies in Engineering Failure Analysis*, **9**, 35 (2017). Doi: https://doi.org/10.1016/j.csefa.2017.06.002
10. M. C. Fatah, D. T. Putra, and B. A. Kurniawan, Failure investigation of high temperature cast soot blower lance tube nozzle, *Journal of Failure Analysis and Prevention*, **20**, 1124 (2020). Doi: https://doi.org/10.1007/s11668-020-00914-w